

Generation of structure light in probe absorption spectrum via microwave-driven Y-type atomic system

Muhammad Saeed and Muqaddar Abbas
Citation: Chin. Phys. B, 2023, 32 (**12**): 124211. DOI: 10.1088/1674-1056/aceee7
Journal homepage: http://cpb.iphy.ac.cn; http://iopscience.iop.org/cpb

What follows is a list of articles you may be interested in

Theoretical analysis of the optical rotational Doppler effect under atmospheric turbulence by mode decomposition

Sheng-Jie Ma(马圣杰), Shi-Long Xu(徐世龙), Xiao Dong(董骁), Xin-Yuan Zhang(张鑫源), You-Long Chen(陈友龙), and Yi-Hua Hu(胡以华)
Chin. Phys. B, 2023, 32 (**10**): 104208. DOI: 10.1088/1674-1056/acc1d0

Ultraviolet metalens and metalens array of focused vortex beams

Jinping Zhang(张金平), Yan Wang(王焱), Huan Yuan(袁欢), Zehao Wang(王泽豪), Yang Deng(邓阳),Chengzhi Huang(黄承志), Jiagui Wu(吴加贵), and Junbo Yang(杨俊波)
Chin. Phys. B, 2023, 32 (**6**): 064206. DOI: 10.1088/1674-1056/ac9d87

Propagation and focusing characteristics of the Bessel-Gaussian beam with the spiral phase term of new power-exponent-phase

Aotian Wang(王傲天), Lianghong Yu(於亮红), Jinfeng Li(李进峰), and Xiaoyan Liang(梁晓燕)
Chin. Phys. B, 2023, 32 (**4**): 044201. DOI: 10.1088/1674-1056/acb1fe

Generation of elliptical airy vortex beams based on all-dielectric metasurface

Xiao-Ju Xue(薛晓菊), Bi-Jun Xu(徐弼军), Bai-Rui Wu(吴白瑞), Xiao-Gang Wang(汪小刚), Xin-Ning Yu(俞昕宁), Lu Lin(林露), and Hong-Qiang Li(李宏强)
Chin. Phys. B, 2023, 32 (**2**): 024215. DOI: 10.1088/1674-1056/ac7cd0

Tightly focused properties of a partially coherent radially polarized power-exponent-phase vortex beam

Kang Chen(陈康), Zhi-Yuan Ma(马志远), and You-You Hu(胡友友)
Chin. Phys. B, 2023, 32 (**2**): 024208. DOI: 10.1088/1674-1056/ac70b0

Generation of structure light in probe absorption spectrum via microwave-driven Y-type atomic system

Muhammad Saeed[1] and Muqaddar Abbas[2,†]

[1] *Center for Integrated Quantum Information Technologies (IOIT), School of Physics and Astronomyand State Key Laboratory of Advanced Optical Communication Systems and Networks, Shanghai Jiao Tong University, Shanghai* 200240, *China*

[2] *Key Laboratory for Nonequilibrium Synthesis and Modulation of Condensed Matter (Ministry of Education), Shaanxi Province Key Laboratory of Quantum Information and Quantum Optoelectronic Devices, School of Physics, Xi'an Jiaotong University, Xi'an* 710049, *China*

(Received 18 June 2023; revised manuscript received 3 August 2023; accepted manuscript online 10 August 2023)

Behavior of structure light is investigated by monitoring probe absorption using a microwave-driven Y-type atomic media configuration. The system under consideration is driven by one of the control vortex beams as well as an extra non-vortex control beam to ensure electromagnetically induced transparency. The significant aspect in the generation of structured light is the azimuthal phase-dependent modification for probe absorption. Further intensity distribution for absorption spectra is examined for simultaneously evaluating both the control vortex beams. We also go through the radial distribution of intensity for various orbital angular momentum values. Different modes of structural beams may be distinguished using the suggested approach. Our research gives us a way for rapidly transferring vortex wavefronts from control field to probe absorption profile. This could be useful in quantum information processing.

Keywords: structure light, vortex beam

PACS: 42.50.–p, 32.80.Qk, 42.50.Ct, 34.80.Pa **DOI:** 10.1088/1674-1056/aceee7

1. Introduction

Interference and atomic coherence are two basic phenomena that can influence spectrum features of a multilayer atomic system. In a broader sense, quantum interference occurs when there are two or more indistinguishable transition routes.[1–3] Normally opaque materials may become completely transparent to a probe beam via the quantum interference phenomena of electromagnetically induced transparency (EIT). The destructive interference across the probe absorption amplitudes causes such transparency. Boller *et al.* initially demonstrated it experimentally in 1991,[4] EIT has resulted in increasing interests for scientific research. One of the notable consequences of EIT is the ability to slow down or completely halt light propagation many times.[5–9]

In recent years, researchers have examined that the average velocity of the group associated with a pulse of light can be reduced to 17 m/s in the Bose–Einstein condensate of sodium atom gas.[6] In literature, there has been a lot of research on EIT in V, Λ, along with cascade (ladder) atomic systems with three levels.[10–12] Comparatively minimal research in both theory and experiment concerning the Y-type atomic structure[10,13–15] has ever been carried out. Hou *et al.*[10,13] inquired into how vacuum-induced coherence (VIC) affects the absorbance properties of Y-type atomic structures. The effect of VIC on absorption features of incoherent pumping field for Y-type four-level systems was studied.[14] Moreover, two photons absorbed in sodium vapor were suppressed by electromagnetic interference according to Gao *et al.*[15] The effect for a single strong coupling field generates an EIT window inside the probe field's absorption profile, allowing subluminal light passage, as shown by using three-level atomic systems. However, because of the extra (second) pumping field coupling with four-level atomic arrangement, an additional EIT window may exist as well as be altered as compared to a three-level atomic structure. Several practical and theoretical studies have been conducted on such a double EIT system since it may improve non-linear optical effects when compared to single EIT structures.[16,17]

Light may have both spin angular momentum (SAM) and orbital angular momentum (OAM), with SAM related with light polarization and OAM associated with helical phase vortices $e^{il\Phi}$. In this case, l represents the topological charge, also known to be the winding number, along with the azimuthal quantum number. Allen and colleagues discovered the Laguerre–Gaussian (LG) modes, which are characteristic manifestations of light with OAM.[18] The LG beam's pattern of intensity distribution is doughnut-shaped, exhibiting zero intensity at the center. Light having OAM (structured light) provides potential use in quantum information,[19] as well as optical communications,[20,21] optical trapping,[22,23] and optical tweezers[24] because of the intensity as well as phase structure's specific features. Structured light interactions with atomic ensembles have been studied for a variety of applications by researchers.[25–30] Light beams with spatial structure may be employed in applications for optically sensing. In particular, the rotational Doppler effect may be used to measure

†Corresponding author. E-mail: muqaddarabbas@xjtu.edu.cn

© 2023 Chinese Physical Society and IOP Publishing Ltd

the rotation of objects along with particles.[31,32] Additionally, structured light pulses having discrete phase patterns as well as intensity distributions are employed in imaging applications, such as fiber endoscopes[33] along with super-resolution imaging.[34]

EIT-based structured generation of light has been considered by employing closed three-level[35] as well as four-level atomic setups.[36,37] For the experimental demonstration of the vortex beam, researchers manipulated a structured probe beam with a transverse magnetic field in rubidium atoms.[36] A tripod along with Λ-type atomic setup has also been used to examine a structured light in a five-level atomic system.[38] Also, researchers considered the probing field including non-vortex, while the control field including OAM.[39–43] The phenomenon is most expected because an auxiliary field without a vortex is required for maintaining EIT when the driving fields include OAM since the optical vortex's center has zero intensity.[44] Additionally, using two-component slow light[45] as well as four-wave mixing using a double-Λ configuration,[46] it has been suggested that optical vortices in a double tripod atomic structure might be transported from the control to the probe beam. Due to EIT's success and importance in resonant atomic systems, practical and theoretical research into its use in semiconductor devices has been sparked.

In this work, we analyze a weak probing field, and two coherent coupling fields, alongside a four-level Y-type atomic system. We look at how the coupling field detuning as well as Rabi frequencies influences the probe field's dispersion as well as absorption in such a system. We show spatially structure arising to absorption profile and how their presence can be explained by applying LG vortex to upper levels dressed state representations as well as their transitions to the lowest level.

2. Theory formulation

2.1. Y-type atomic system driven by a microwave field

Let us start by presenting the Y-type model system examined in the present study and shown in Fig. 1(a). Phase profile of the LG beam with $l = 4$ is shown in Fig. 1(b). The structure of this model includes the ground level $|0\rangle$, a level that is intermediate $|1\rangle$, and two higher levels $|2\rangle$ and $|3\rangle$, which may be energy close or even (almost) degenerate. A weak and adjustable probe laser field associated with Rabi frequency $\Omega_{\rm p}$ couples to the level $|0\rangle$ along with $|1\rangle$, whereas the level in middle $|1\rangle$ connects to levels $|2\rangle$ and $|3\rangle$ via two distinct tunable coupling fields along with the Rabi frequencies Ω_1 and Ω_2, respectively.

With the exception of the bottom level, each level will deteriorate by spontaneous photon emission at the showed decay rates, which are γ_1, γ_2, and γ_3. As usual, we assume that because of their parities as well as total angular momenta, the higher levels $|2\rangle$ and $|3\rangle$ only decay to the intermediate level $|1\rangle$. This kind of Y-type model system can be approximated, for instance, in rubidium vapor through recognizing the $(4p^6 5s)^2S_{1/2}$ neutral rubidium at ground level using $|0\rangle$, the $(4p^6 5p)^2P_{3/2}$ with level $|1\rangle$ as well as the two $(4p^6 5d)^2D_{3/2,5/2}$ levels correspond to excited levels $|2\rangle$ and $|3\rangle$. In an interaction diagram, the total Hamiltonian for a Y-type system influenced by a microwave field reads

$$\begin{aligned} H_I &= \hbar(\Delta_{\rm p}|1\rangle\langle 1| - (\Delta_{\rm p}+\Delta_1)|2\rangle\langle 2| \\ &\quad -(\Delta_{\rm p}+\Delta_2)|3\rangle\langle 3|) - \hbar(\Omega_{\rm p}|0\rangle\langle 1| \\ &\quad +\Omega_1|1\rangle\langle 2| + \Omega_2|1\rangle\langle 3| + \Omega_{\rm B}|2\rangle\langle 3| + {\rm H.c.}). \end{aligned} \tag{1}$$

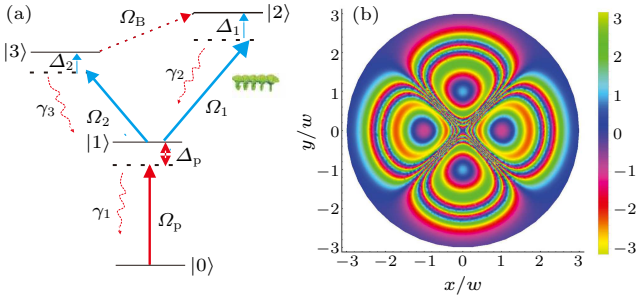


Fig. 1. (a) Diagrammatic illustration of a four-level closed Y-type atomic system. $\Omega_{\rm p}$, Ω_1, Ω_2 and $\Omega_{\rm B}$ represent the Rabi frequencies associated with the probe, LG, control and microwave fields. (b) Phase profile of the LG beam with $l = 4$.

The detunings are defined as $\Delta_{\rm p} = \omega_{10} - \omega_{\rm p}$, $\Delta_1 = \omega_{31} - \omega_1$, and $\Delta_2 = \omega_{21} - \omega_2$. Employing the Liouville equation, we can derive the subsequent rate equations over the density matrix constituents as follows:

$$\begin{aligned} \dot{\rho}_{10}^{(1)} &= \Gamma_{10}\rho_{10} - {\rm i}\Omega_1\rho_{20} - {\rm i}\Omega_2\rho_{30} - {\rm i}\Omega_{\rm p}, \\ \dot{\rho}_{20}^{(1)} &= \Gamma_{20}\rho_{20} - {\rm i}\Omega_1\rho_{10} - {\rm i}\Omega_{\rm m}\rho_{30}, \\ \dot{\rho}_{30}^{(1)} &= \Gamma_{30}\rho_3 - {\rm i}\Omega_2\rho_{10} - {\rm i}\Omega_{\rm m}\rho_{20}, \end{aligned} \tag{2}$$

where $\Gamma_{10} = {\rm i}\Delta_{\rm p} - \gamma_1$, $\Gamma_{20} = {\rm i}(\Delta_{\rm p}+\Delta_1) - \gamma_2$, and $\Gamma_{30} = {\rm i}(\Delta_{\rm p} + \Delta_2) - \gamma_3$. Also, γ_i $(i = 1,2,3)$ are actually the rates of spontaneous decay from an excited state $|1\rangle$ pertaining to the ground state $|0\rangle$, also $|2\rangle$ to $|1\rangle$, along with $|3\rangle$ to $|1\rangle$ as shown in Fig. 1(a). To resolve Eq. (2), we assume perturbation theory under a steady-state condition. In the subsequent calculations, we maintain the terms of the density-matrix equations up to the first order. When the field is inadequate enough, only the first-order term matters. We solve Eq. (2) considering $\dot{\rho}_{ij} = 0$ and obtain $\rho_{10}^{(1)}$ as follows:

$$\begin{aligned} \rho_{10}^{(1)} = \Big[{\rm i}(\Gamma_{20}\Gamma_{30} + |\Omega_{\rm m}|^2)\Omega_{\rm p}\Big] \Big/ \Big[\Gamma_{10}\Gamma_{20}\Gamma_{30} + \Gamma_{30}|\Omega_1|^2 \\ - {\rm i}\Omega_1^*\Omega_{\rm m}\Omega_2 + \Gamma_{20}|\Omega_2|^2 + \Gamma_{10}|\Omega_{\rm m}|^2 - {\rm i}\Omega_1\Omega_2^*\Omega_{\rm m}\Big]. \end{aligned} \tag{3}$$

2.2. Control vortex fields

The light beams are LG doughnut type beams. In terms of Rabi-frequencies, these LG beams are defined as

$$\Omega_{(1,2)} = \varepsilon_{(1,2)} \left(\frac{r_{(1,2)}}{w}\right)^{|l_{(1,2)}|} \mathrm{e}^{-\frac{r^2_{(1,2)}}{w^2}} \mathrm{e}^{\mathrm{i}l_{(1,2)}\Phi_{(1,2)}}, \tag{4}$$

where $\Phi = \tan^{-1}(y/x)$, $r = \sqrt{x^2+y^2}$, w is the beam waist, and $\varepsilon_{(1,2)}$ is the strength of the beam.

2.3. Azimuthal modulation for absorption of the probe with one control beam as a structure beam

The value of the $\rho_{10}^{(1)}$ is a complex number with both real and imaginary parts. The real part is connected to dispersion, whereas the imaginary part relates to probing field absorption. In this section, we simply look at the imaginary component of $\rho_{10}^{(1)}$ and explore the absorbing profile for the probe field associated with the atomic transition $|0\rangle \longleftrightarrow |1\rangle$. First, we look at how the azimuthal angle affects the absorption pattern generated by the probing field. In such a scenario, one of the control fields Ω_1 carries OAM l_1 as given in Eq. (4), whereas the remaining fields have no vortices. We depict the probing field absorption profile against azimuthal angle Φ for OAM, $l_1 = 4$ in Fig. 2(a). The remaining parameters are $\gamma = 1$ MHz, $\gamma_1 = 0.5\gamma$, $\gamma_2 = 0.01\gamma$, $\gamma_3 = 0.01\gamma$, $\Omega_\mathrm{m} = 0.1\gamma$, $\Omega_\mathrm{p} = 0.1\gamma$, $\Omega_2 = 0.5\gamma$, $\Delta_\mathrm{p} = \Delta_1 = \Delta_2 = 0$. At varying azimuthal angles Φ, we observe optical transparency ($\mathrm{Im}[\rho_{10}^{(1)}] = 0$), and absorption ($\mathrm{Im}[\rho_{10}^{(1)}] > 0$). As illustrated in Fig. 2(a), there is absorption and transparency at certain azimuthal phases for $l_1 = 4$. Figure 2(b) depicts intensity at various Φ, such as 0, π, and 2π. By raising the OAM from $l_1 = 4$, Fig. 2(b) shows absorption and transparency that show spatial dependence. To investigate spatially modifying probe field absorption, we use a Rabi frequency Ω_1 control field as a vortex doughnut type beam provided by Eq. (4). The rest of the fields are without Φ (azimuthal angle). Because intensity becomes zero for the vortex beam at $r \to 0$ [see Fig. 1(b)], EIT disappears at the center of the vortex beam in a three-level atomic system. When $\Omega_1 = 0$, Eq. (3) simplifies to

$$\rho_{10}^{(1)} = \frac{\mathrm{i}(\Gamma_{20}\Gamma_{30})\Omega_\mathrm{p}}{\Gamma_{10}\Gamma_{20}\Gamma_{30} + \Gamma_{20}|\Omega_2|^2}, \tag{5}$$

which denotes standard EIT. Thus, to keep EIT even at the center of a vortex beam, we think of one control beam as not being a vortex.

Next, we look into the probe field's absorption pattern for different winding numbers l_1. In Figs. 3(a)–3(d), we can see how the absorption profile changes in various locations when one of the control fields is used as a structure beam for (a) $l_1 = 1$, (b) $l_1 = 2$, (c) $l_1 = 3$, and (d) $l_1 = 4$. We can see the spectrum of absorption established against the standardized values x/w and y/w. We see shapes that look like petals, and the number of those petal shapes increases as the winding number enhances. The bright spots show where light is absorbed, and the dark show where light can transmit through. Based on the above results, it seems that the OAM l_1 affects how the probe field's absorption profile changes.

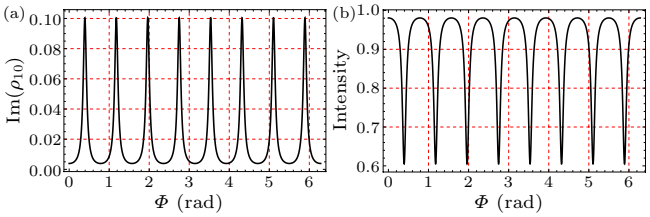


Fig. 2. (a) Pattern of absorption versus azimuthal angle Φ, (b) intensity pattern versus azimuthal angle Φ. Here $l_1 = 4$, $\Omega_\mathrm{p} = 0.1\gamma$, and $\Omega_\mathrm{B} = 0.1\gamma$.

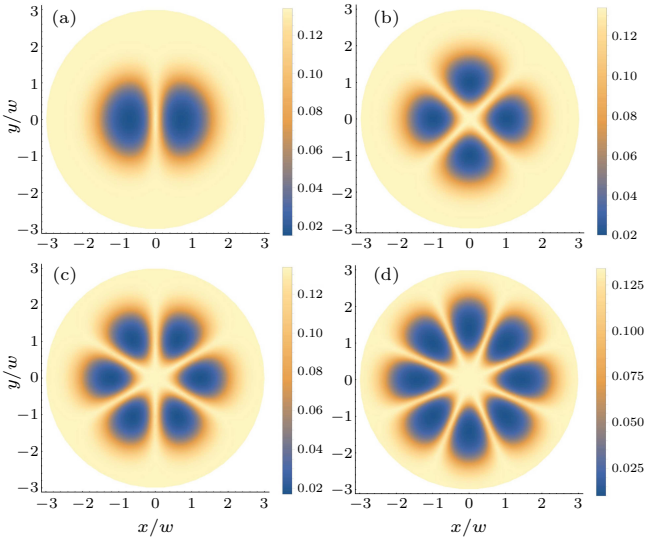


Fig. 3. Pattern of absorption versus x/w and y/w for (a) $l_1 = 1$, (b) $l_1 = 2$, (c) $l_1 = 3$, and (d) $l_1 = 4$. The rest of parameters are $\gamma = 1$ MHz, $\gamma_1 = 0.5\gamma$, $\gamma_2 = 0.01\gamma$, $\gamma_3 = 0.01\gamma$, $\Omega_\mathrm{m} = 0.1\gamma$, $\Omega_\mathrm{p} = 0.1\gamma$, $\Omega_2 = 0.5\gamma$, and $\Delta_\mathrm{p} = \Delta_1 = \Delta_2 = 0$.

We did not take into account the Doppler effect when we used density matrix theory to figure out the physical response of the medium. Measurements were carried out by considering ^{87}Rb atoms in the magneto-optical trap (MOT) that is used to trap and cool atoms in this kind of setting. To decrease the Doppler broadening effect, the counter-propagating beam method can be used to analyze hot atomic media.[47] On the other hand, using cold atoms is the best way to avoid the Doppler effect.[48]

2.4. Transfer of optical vortices by considering both control fields as vortex beam

In this subsection, we show how optical vortices may be transferred through the control field to that of the probe field. We now assume that both control fields contain vortex beams as given in Eq. (4). The probing field's time-independent transmission equation under slowly changing envelop assumptions may be given as

$$\frac{\partial \Omega_\mathrm{p}(z)}{\partial z} = -\mathrm{i}\frac{\alpha_\mathrm{p}\gamma_1}{2L}\rho_{10}^{(1)}, \tag{6}$$

as $\alpha_{\rm p}$ signifies the optical depth for the probe field, and L represents the atomic vapor cell length. A transmitted probing field may be expressed using Eq. (4) as

$$\Omega_{\rm p}(z) = \Omega_{\rm p}(0)\,{\rm e}^{\kappa z}, \tag{7}$$

where $\Omega_{\rm p}(0)$ represents the probe field at the cell's entrance while

$$\kappa = \frac{\alpha_{\rm p}\gamma_1}{2L}\cdot[{\rm i}(\Gamma_{20}\Gamma_{30}+|\Omega_{\rm m}|^2)]\cdot\{\Gamma_{10}\Gamma_{20}\Gamma_{30}+\Gamma_{30}|\Omega_1|^2 -{\rm i}\Omega_1^*\Omega_{\rm m}\Omega_2+\Gamma_{20}|\Omega_2|^2+\Gamma_{10}|\Omega_{\rm m}|^2-{\rm i}\Omega_1\Omega_2^*\Omega_{\rm m}\}^{-1}. \tag{8}$$

We examine control fields E_1 and E_2, which both carry the OAM and have corresponding Rabi frequencies Ω_1 and Ω_2 with vortices l_1 and l_2. According to Eq. (7) OAM l_1 (l_2) of pump field Ω_1 (Ω_2) has been transferred via the transmitting probing field. At the atomic medium's entrance, the incoming probe field does not impart any vortex. The vortex of the control beams transfers to the probe beam after some distance due to the atomic system's closed-loop construction. We depict the intensity pattern for the transmitting probe field at $z = L$ in Figs. 4(a)–4(d), for $l_1 = l_2 = 1,2,3,4$ as well as $\alpha_{\rm p} = 100$. The intensity patterns depict a doughnut shape with a black zone in the middle displaying zero magnitudes. The central dark zone broadens as the winding number grows, while the associated phases change from 0 to $2\pi l$ within the singularity point.

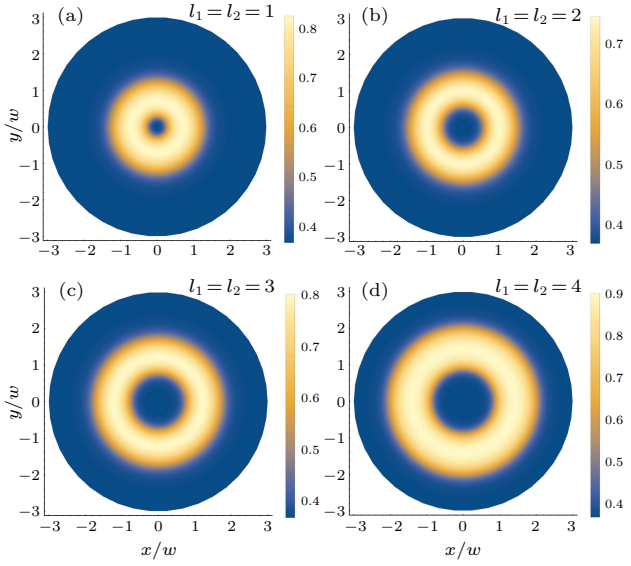


Fig. 4. Intensity pattern versus x/w and y/w for (a) $l_1 = l_2 = 1$, (b) $l_1 = l_2 = 2$, (c) $l_1 = l_2 = 3$, and (d) $l_1 = l_2 = 4$. The rest of parameters are $\gamma = 1$ MHz, $\gamma_1 = 0.5\gamma$, $\gamma_2 = 0.01\gamma$, $\gamma_3 = 0.01\gamma$, $\Omega_{\rm m} = 0.1\gamma$, $\Omega_{\rm p} = 0.1\gamma$, $\Omega_2 = 0.5\gamma$, and $\Delta_{\rm p} = \Delta_1 = \Delta_2 = 0$.

In Fig. 5, we plot intensity versus radial distance r/w for winding numbers (a) $l_1 = l_2 = 1$, (b) $l_1 = l_2 = 2$, (c) $l_1 = l_2 = 3$, and (d) $l_1 = l_2 = 4$. The degree of intensity is highest at $r = 0.8w$ and zero at $r > 1.2w$ and $r < 0.4w$ for $l_1 = l_2 = 1$ as well as $l_1 = l_2 = 2$, as shown in Figs. 5(a)–5(d). In order to acquire a physical understanding for this phenomenon, we first investigate the case in which Ω_2 is not present.

Our original Y-type system is reduced to a ladder-type three-level configuration design in this scenario. In the presence of Ω_1, the transmission of $\Omega_{\rm p}$ rises owing to EIT. Whenever Ω_2 is present, however, EIT becomes of interference and probe field absorption rises. As a result, Ω_1 pumps the population to the excited state $|2\rangle$. The magnetization field $\Omega_{\rm m}$ generates nonlinearity within the population, causing the intensity of its absorption profile to become spatially dependent at a particular radial distance. Assuming that Ω_1 and Ω_2 are vortex fields with decreasing intensities when approached by $r > 1.2w$ and $r < 0.4w$, respectively, see Figs. 5(a) and 5(b), the dark state formed in the presence of Ω_1 is disrupted and the conversion intensity drops. The same is true for $l_1 = l_2 = 3$ and $l_1 = l_2 = 4$, as illustrated in Figs. 5(c) and 5(d).

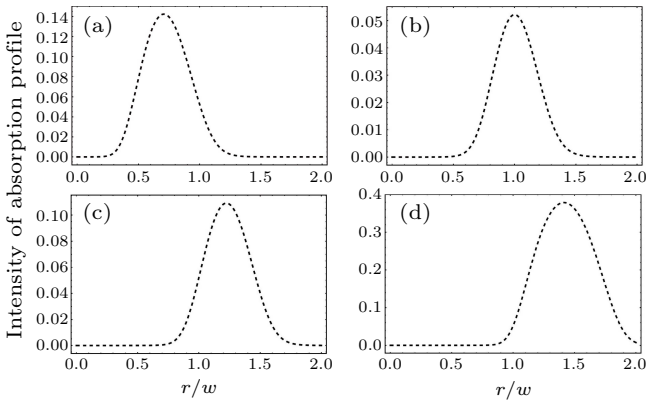


Fig. 5. The intensity of the spectrum of absorption against the radial distance r/w for (a) $l_1 = l_2 = 1$, (b) $l_1 = l_2 = 2$, (c) $l_1 = l_2 = 3$, and (d) $l_1 = l_2 = 4$. The remaining parameters remain same as in Fig. 4.

3. Experimental realization of our proposed system

Our proposed method may be examined experimentally for the generation of structure light employing cold ^{8}7Rb atoms through probe absorption[49,50] using the transitions $5S_{1/2}$–$5P_{3/2}$–$5D_{5/2,3/2}$. Following states may be designated as: $|0\rangle = |5S_{1/2}, F = 2\rangle$, $|1\rangle = |5P_{3/2}, F = 3\rangle$, $|2\rangle = |5D_{5/2}, F = 4\rangle$, and $|3\rangle = |5D_{3/2}, F = 3\rangle$. In the present situation, the decay rates of the excited along with intermediate states are $\gamma_1 = 0.5$ MHz as well as $\gamma_2 = \gamma_3 = 0.01$ MHz. In realistic investigations, Ω_1 couples with atomic transitions in an approximate wavelength of 776.2 nm, whereas Ω_2 couples in a wavelength of 775.8 nm. All of them can be generated using diode lasers. Here, the control field Ω_1 interacts via transition $|5P_{3/2}, F = 3\rangle \longleftrightarrow |5D_{5/2}, F = 4\rangle$ and Ω_2 interacts alongside the transition $|5P_{3/2}, F = 3\rangle \longleftrightarrow |5D_{3/2}, F = 3\rangle$. Next we consider one of the control field as vortex beam that is generated by spatial light modulator,[51] and examine the generation of structured light for probe absorption. Further, we consider both control vortex beams and see the intensity profile of the generated structure beam. In each scenario, the weak probe field interacts via transition $|5S_{1/2}, F = 2\rangle \longleftrightarrow |5P_{3/2}, F = 3\rangle$

and hyperfine transition $|5D_{5/2}, F = 4\rangle \longleftrightarrow |5D_{3/2}, F = 3\rangle$ associated through a microwave-driven field with frequency that is around 100 GHz. We expect that our proposed system can be realized experimentally by considering the above-mentioned parameters and approach.

4. Conclusion

In summary, we have explored spatial transparency in a Y-type atomic setup with two pump fields, a probe, as well as a microwave field. A vortex-based beam is utilized to periodically modulate the absorbing profile within its azimuthal region. This periodic oscillation is the main reason for structured light generation. The absorption profile exhibits $2\pi l$-fold symmetry, along with the OAM coupled with a vortex-type beam in a petal-like shape that varies with increasing winding number identified. It is also feasible to transfer the OAM from controlling the vortices beam to the transmitted probing beam. By considering both controlling fields as vortex beams, we see the intensity of probe field that has a doughnut shape. The size of the dark region increases with the increase of winding number. Lastly, we see the radial distance effect on the intensity of probe field. The intensity increases for a certain radial distance and then decreases as the dark state is created. Our suggested approach may pave the way for further research of applications in telecommunications and optical information processing.

References

[1] Scully M O and Zubairy M S 1997 *Quantum Optics* (Cambridge: Cambridge University Press)
[2] Safari L, Amaro P, Fritzsche S, Santos J P and Fratini F 2012 *Phys. Rev. A* **85** 043406
[3] Safari L, Amaro P, Fritzsche S, Santos J P, Tashenov S and Fratini F 2012 *Phys. Rev. A* **86** 043405
[4] Boller K J, Imamoglu A and Harri S E Phys 1991 *Phys. Rev. Lett.* **66** 2593
[5] Akulshin A M, Cimmino A, Sidorov A I, Hannaford P and Opat G I 2003 *Phys. Rev. A* **67** 011801
[6] Hau L V, Harris S E, Dutton Z and Behroozi C H 1999 *Nature* **397** 594
[7] Wu B, Hulbert J F, Lunt E J, Hurd K, Hawkins A R and Schmidt H 2010 *Nat. Photon.* **4** 776
[8] Bigelow M S, Lepeshkin N N and Boyd R W 2003 *Science* **301** 200
[9] Bajcsy M, Zibrov A S and Lukin M D 2003 *Nature* **426** 638
[10] Hou B P, Wang S J, Yu W L and Sun W L 2004 *Phys. Rev. A* **69** 053805
[11] Mitra S, Dey S, Hossain M M, Ghosh P N and Ray B 2013 *J. Phys. B* **46** 075002
[12] Xiao M, Li Y Q, Jin S Z and Gea-Banacloche J 1995 *Phys. Rev. Lett.* **74** 666
[13] Hou B P, Wang S J, Yu W L and Sun W L 2005 *J. Phys. B: At. Mol. Opt. Phys.* **38** 1419
[14] Dutta B K and Mahapatra P K 2008 *J. Phys. B: At. Mol. Opt. Phys.* **41** 055501
[15] Gao J Y, Yang S H, Wang D, Guo X Z, Chen K X, Jiang Y and Zhao B 2000 *Phys. Rev. A* **61** 023401
[16] Zhang Y, Brown A W and Xiao M 2007 *Phys. Rev. Lett.* **99** 123603
[17] Liu Y, Wu J, Ding D, Shi B and Guo G 2012 *New J. Phys.* **14** 073047
[18] Allen L, Beijersbergen M W, Spreeuw R J C and Woerdman J P 1992 *Phys. Rev. A* **45** 8185
[19] Dada A C, Leach J, Buller G S, Padgett M J and Andersson E 2011 *Nat. Phys.* **7** 677
[20] Wang J, Yang J Y, Fazal I M, Ahmed N, Yan Y, Huang H, Ren Y, Yue Y, Dolinar S, Tur M and Willner A E 2012 *Nat. Photon.* **6** 488
[21] Bozinovic N, Yue Y, Ren Y X, Tur M, Kristensen P, Huang H, Willner A E and Ramachandran S 2013 *Science* **340** 1545
[22] Friese M E J, Enger J, Rubinsztein-Dunlop H and Heckenberg N R 1996 *Phys. Rev. A* **54** 1593
[23] Garcés-Chávez V, McGloin D, Padgett M J, Dultz W, Schmitzer H and Dholakia K 2003 *Phys. Rev. Lett.* **91** 093602
[24] Padgett M J and Bowman R 2011 *Nat. Photon.* **5** 343
[25] Chanu S R and Natarajan V 2013 *Opt. Commun.* **295** 150
[26] Ding D S, Zhang W, Zhou Z Y, Shi S, Xiang G Y, Wang X S, Jiang Y K, Shi B S and Guo G C 2015 *Phys. Rev. Lett.* **114** 050502
[27] Dholakia K, Simpson N B, Padgett M J and Allen L 1996 *Phys. Rev. A* **54** R3742
[28] Courtial J, D holakia K, Allen L and Padgett M J 1997 *Phys. Rev. A* **56** 4193
[29] Walker G, Arnold A S and Franke-Arnold S 2012 *Phys. Rev. Lett.* **108** 243601
[30] Persuy D, M. Ziegler, Crégut O, Kheng K, Gallart M, Hönerlage B and Gilliot P 2015 *Phys. Rev. B* **92** 115312
[31] Lavery M P, Speirits F C, Barnett S M and Padgett M J 2013 *Science* **341** 537
[32] Fang L, Padgett M J and Wang J 2017 *Laser Photon. Rev.* **11** 1770064
[33] Plöschner M, Tyc T and Cižmár T 2015 *Nat Photon.* **9** 529
[34] Kozawa Y, Matsunaga D and Sato S 2018 *Optica* **5** 86
[35] Han L, Cao M, Liu R, Liu H, Guo W, Wei D, Gao S, Zhang P, Gao H and Li F 2012 *Eur. Phys. Lett.* **99** 34003
[36] Radwell N, Clark T W, Piccirillo B, Barnett S M and Franke-Arnold S 2015 *Phys. Rev. Lett.* **114** 123603
[37] Sharma S and Dey T N 2017 *Phys. Rev. A* **96** 033811
[38] Hamedi H R, Kudriašov V, Ruseckas J and Juzeliūnas G 2018 *Opt. Express* **26** 28249
[39] Duttonand Z and Ruostekoski J 2004 *Phys. Rev. Lett.* **93** 193602
[40] Pugatch R, Shuker M, Firstenberg O, Ron A and Davidson N 2007 *Phys. Rev. Lett.* **98** 203601
[41] Wang T, Zhao L, Jiang L and Yelin S F 2008 *Phys. Rev. A* **77** 043815
[42] Xie X T, Li W B and Yang X 2006 *J. Opt. Soc. Am. B* **23** 1609
[43] Moretti D, Felinto D and Tabosa J W R 2009 *Phys. Rev. A* **79** 023825
[44] Ruseckas J, Mekys A and Juzeliūnas G 2011 *Phys. Rev. A* **83** 023812
[45] Ruseckas J, Kudriašov V, Yu I A and Juzeliūnas G 2013 *Phys. Rev. A* **87** 053840
[46] Hamedi H R, Ruseckas J and Juzeliūnas G 2018 *Phys. Rev. A* **98** 013840
[47] Ye C Y, Zibrov A S, Rostovtsev Y V and Scully M O 2002 *Phys. Rev. A* **65** 043805
[48] Uhlenberg G, Dirscherl J and Walther H 2000 *Phys. Rev. A* **62** 063404
[49] Noh H R and Moon H S 2011 *Opt. Express* **19** 11128
[50] Zhang Y P, Brown A W and Xiao M 2007 *Phys. Rev. Lett.* **99** 123603
[51] Ostrovsky A S, Rickenstorff-Parrao C and Arrizón V 2013 *Opt. Lett.* **38** 534